Journal Pre-proofs

Design, synthesis, and computational validation of novel compounds selectively targeting HER2-expressing breast cancer

Samia A. Elseginy, Rania Hamdy, Varsha Menon, Ahmed M. Almehdi, Raafat El-Awady, Sameh Soliman

PII: S0960-894X(20)30769-1
DOI: https://doi.org/10.1016/j.bmcl.2020.127658
Reference: BMCL 127658

To appear in: *Bioorganic & Medicinal Chemistry Letters*

Received Date: 22 August 2020
Revised Date: 7 October 2020
Accepted Date: 25 October 2020

Please cite this article as: Elseginy, S.A., Hamdy, R., Menon, V., Almehdi, A.M., El-Awady, R., Soliman, S., Design, synthesis, and computational validation of novel compounds selectively targeting HER2-expressing breast cancer, *Bioorganic & Medicinal Chemistry Letters* (2020), doi: https://doi.org/10.1016/j.bmcl.2020.127658

Design, synthesis, and computational validation of novel compounds selectively targeting HER2-expressing breast cancer

Samia A. Elseginy[a,b], Rania Hamdy[c,d], , Varsha Menon[c], Ahmed M. Almehdi[e], Raafat El-Awady[c,f], Sameh Soliman[e,f*]

[a]Green Chemistry Department, Chemical Industries Research Division, National Research Center P.O. Box 12622, Egypt
[b]Molecular Modelling Lab., Biochemistry School, Bristol University, Bristol, UK
[c]Research Institute for Medical and Health Sciences, University of Sharjah, P.O. Box 27272, Sharjah, UAE
[d]Faculty of Pharmacy, Zagazig University, Zagazig, 44519, Egypt
[e]College of Sciences, University of Sharjah, P.O. Box 27272, Sharjah, UAE
[f]College of Pharmacy, University of Sharjah, P.O. Box 27272, Sharjah, UAE

***Correspondence:**

Sameh Soliman

Department of Medicinal Chemistry, College of Pharmacy

University of Sharjah, Sharjah, UAE, 27272

Phone: +971650 57472, ssoliman@sharjah.ac.ae

Abstract

Human epidermal growth factor receptor (HER) is a family of multidomain proteins that plays important role in the regulation of several biological functions. HER2 is a member of HER that is highly presented in breast cancer cells. Here, we designed and synthesized a series of diaryl urea/ thiourea compounds. The compounds were tested on $HER2^+$ breast cancer cells including MCF-7 and SkBr3, compared to $HER2^-$ breast cancer cells including MDA-MB-231 and BT-549. Only compounds 12-14 at 10μM showed selective anti-proliferative activity against MCF-7 and SkBr3 by 65-79%. Compounds 12-14 showed >80% inhibition of the intracellular kinase domain of HER2. The results obtained indicated that compounds 12-14 are selectively targeting $HER2^+$ cells. The IC_{50} of compound 13 against MCF-7 and SkBR3 were 1.3±0.009 and 0.73±0.03 μM, respectively. Molecular docking and MD simulations (50ns) were carried out, and their binding free energies were calculated. Compounds 12-14 formed strong hydrogen bond and pi–pi stacking interactions with the key residues Thr862 and Phe864. 3DQSAR model confirmed the role of 3-bromo substituent of pyridine ring and 4-chloro substituent of phenyl ring in the activity of the compounds. In conclusion, novel compounds, particularly **13** were developed selectively against HER2-expressing/ overexpressing breast cancer cells including MCF7 and SkBr3.

Keywords: Anticancer drugs; Breast cancers; HER2 targeting; Novel diaryl urea/ thiourea derivatives; Molecular dynamics; Binding energy

Protein kinases play an important role in the signal transduction pathways that regulate various cellular functions including cell proliferation, migration and apoptosis [1]. Signal transduction pathways are unregulated in many cancer cells including breast cancers [2]. Therefore, protein kinases inhibitors are considered as an attractive anticancer candidate. Targeting human epidermal growth factor (HER) by tyrosine kinase inhibitors (TKI) is considered as one of the most promising therapeutic approach [3, 4]. HER receptors are family of multidomain proteins that contain an extracellular ligand binding domain, a single transmembrane domain, and an intracellular tyrosine kinase domain [5]. HER family includes HER1 (ErbB1), HER2 (ErbB2, HER2/ neu), HER3 (ErbB3), and HER4 (ErbB4) [6]. HER2 is overexpressed in a number of human cancers including breast, ovarian, lung, gastric, and oral cancers [7-9], while maintaining low expression levels in normal tissues [10, 11]. This makes HER2 is an attractive target for the development of tumour-specific therapies.

Aryl urea derivatives including diaryl sulphonyl ureas, benzoylureas, and thioureas represent a class of anticancer agents with a wide range of activities against various types of leukaemia and solid tumors [12]. Some aryl urea derivatives have been clinically tested and showed a TKI activity. For example, Sorafenib (**Fig. 1**), developed by Bayer, is used for the treatment of advanced renal cell carcinoma [13]; Linifanib (ABT-869) (**Fig. 1**), developed by Abbott, is currently in phase III clinical trial for the treatment of colorectal cancer [14]. On the other hand, the activity of thiourea derivatives as anticancer agents has inspired the medicinal chemists to design and synthesize new thiourea derivatives with HER2 inhibition activity. Qiu et al., 2010, designed and synthesized 1-(3-chloro-2-hydroxy-benzyl)-1-(4-hydroxy-benzyl)-3-phenyl-thiourea and 1-(3,5-dichloro-2-hydroxy-benzyl)-1-(4-hydroxy-benzyl)-3-phenyl-thiourea [15]. Both compounds showed promising inhibition activity against HER2 receptor at IC_{50} 0.35 and 1.2 µM, respectively. Widiandani et al., 2019, designed 4-*t*-butylbenzoyl-3-allylthiourea, which showed promising anti-proliferation activity against HER2- overexpressing MCF-7 cancer cells [16]. Further, Geogi et al., 2016, synthesized 1-(3-bromo-2-hydroxy-benzyl)-1-(4-fluoro-benzyl)-3-phenyl-thiourea and 1-(3,5-dibromo-2-hydroxy-benzyl)-1-(4-hydroxy-benzyl)-3-phenyl-urea with significant inhibition activity against HER2 at IC_{50} 1.9 and 4.5 µM, respectively [17]. Similarly, we have developed a series of compounds 1-[2-(1H-indol-3-yl) acetyl]-4- arylthiosemicarbazide as dual HER1/ HER2 inhibitors [18]. Based on these data, we have designed and synthesized novel compounds (1-14) by incorporating urea/ thiourea moiety and different lipophilic moieties to enhance the selectivity toward HER2 and the physicochemical characteristics of the compounds. Several computational tools were employed including molecular docking, molecular dynamics, and

calculations of the binding energy. Computational studies indicated the potential activities of the compounds against breast cancer cells with excellent binding affinity to HER2 receptor.

Sorafenib is a multitargeted tyrosine kinase inhibitor (TKI), and the only approved drug for the treatment of hepatocellular carcinoma (HCC), while it shows limited breast cancer efficacy [19]. The combination of Sorafenib with Lapatinib as anti-HER2 agent was investigated as anti-metastatic breast cancer therapy [20]. On the other hand, Linifanib (ABT-869) is a novel receptor tyrosine kinase inhibitor that shows significant activity against HCC. Its combination with Taxol against breast cancer is in clinical trial phase II [14]. Both anticancer drugs, Sorafenib and Linifanib, are 1,3-disubstituted urea that are targeting tyrosine kinase. Inspired with Sorafenib and Linifanib and other previously reported thiourea derivatives with inhibitory activity to HER2 (a receptor tyrosine-protein kinase) [15, 21], we have designed and synthesized a novel series of disubstituted urea and thiourea derivatives. Structural modification by introducing various linkers including CH2, CONH, SO2, NHR, CH2CH2 and/ or different aryl substitutions showed that urea derivatives are less active, while thiourea derivatives (12-14) are more active (**Fig. 1**).

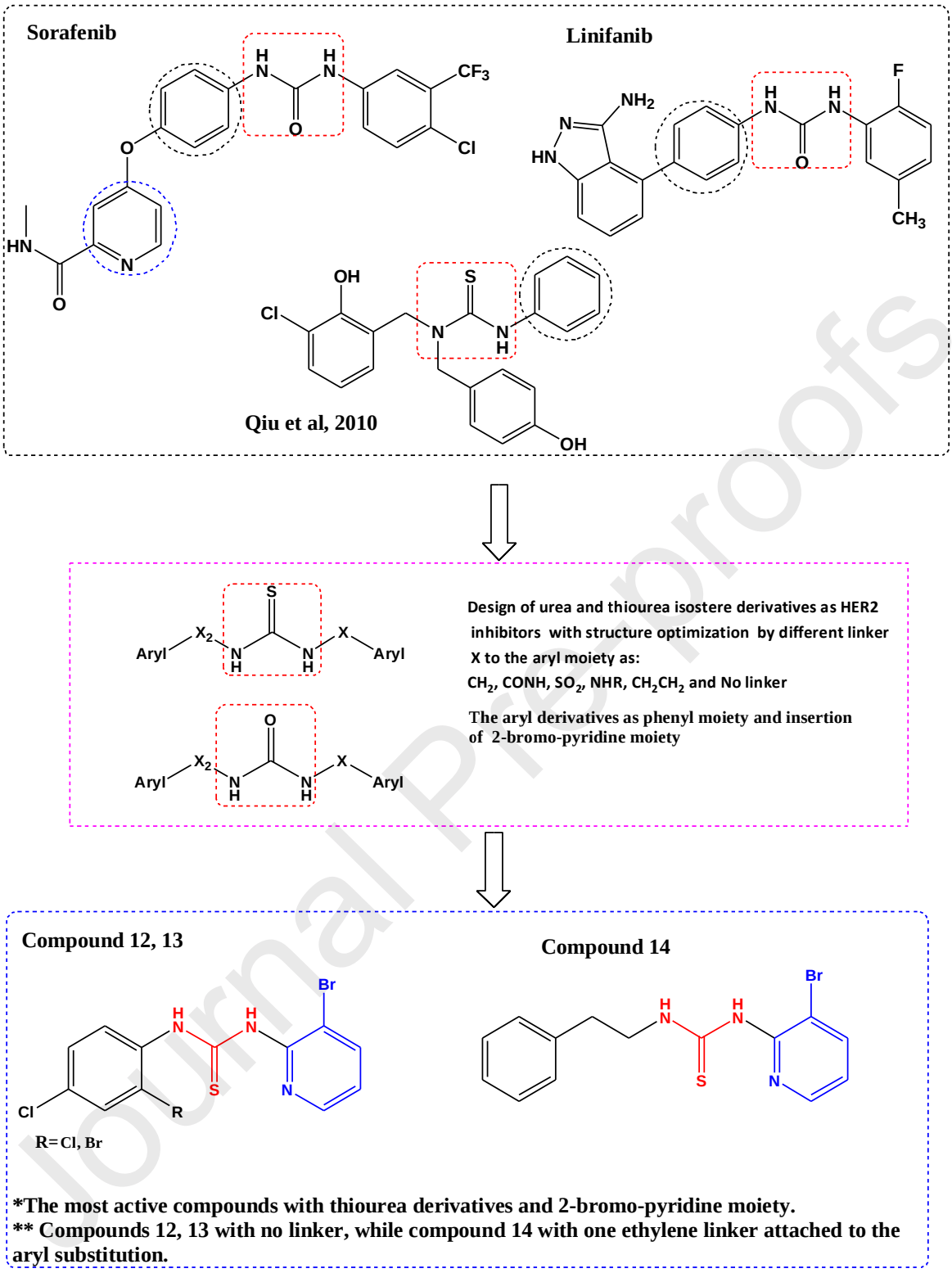

Fig. 1. HER2 inhibitors with urea moiety. Rational design of the HER2 inhibitors with thiourea scaffold based on known HER2 inhibitors with urea scaffold.

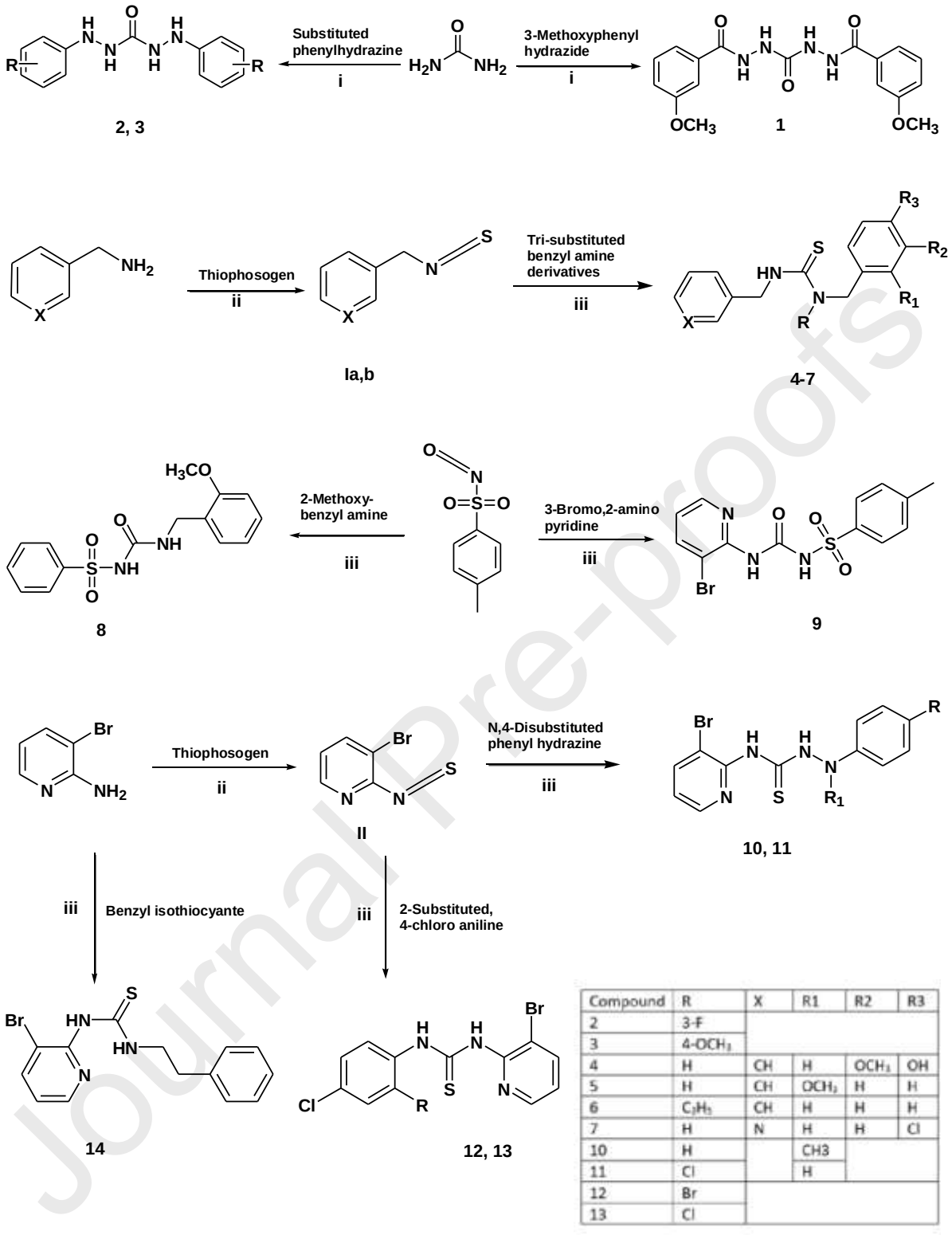

Compound	R	X	R1	R2	R3
2	3-F				
3	4-OCH_3				
4	H	CH	H	OCH_3	OH
5	H	CH	OCH_3	H	H
6	C_2H_5	CH	H	H	H
7	H	N	H	H	Cl
10	H		CH3		
11	Cl		H		
12	Br				
13	Cl				

Fig. 2 (Scheme 1). General scheme for the synthesis of di aryl urea/ thiourea derivatives.

Reagent and condition: i) Ethanol-reflux 24h, ii) CH_2Cl_2/ 0°C, and iii) CH_2Cl_2/ TEA/ 0°C.

The synthesis of diaryl urea/ thiourea derivatives was presented in **Fig. 2** (**Scheme 1**). Diaryl urea derivatives (1-3) were prepared by refluxing urea with hydrazine/ hydrazide derivatives in ethanol for 24 h. The intermediate isothiocyanates derivatives (Ia, Ib and II) were prepared by reacting amine derivatives with thiophosgene in dichloromethane at 0°C. The asymmetrically di-substituted thiourea/ urea compounds were synthesized by reacting the active isothiocyanate derivatives with different aromatic amines. Compounds 4-14 were obtained by stirring isothiocyanate derivatives with the appropriate amine/ hydrazine derivatives in dichloromethane at very low temperature and in the presence of few drops of trimethylamine (TEA).

The anticancer activities of the novel urea/ thiourea derivatives (1-14) were evaluated against human breast cancer cell lines including MCF-7, MDA-MB-231, BT-549 and SkBr3 using the sulforhodamineB assay [22]. The results showed that compounds 12-14 at concentration 10 µM caused remarkable inhibitory activity against SkBR3 (**Fig. 3A** and **Suppl. Table 1**) and MCF-7 cells (**Fig. 3B** and **Suppl. Table 1**). On the other hand, all compounds 1-14 were inactive against MDA-MB-231 and BT-549 cells (**Fig. 3C and D** and **Suppl. Table 1**). Compounds 12-14 caused 74.8%, 79.7% and 78.8% inhibition activity to SkBR3 cells, respectively (**Fig. 3A** and **Suppl. Table 1**) and 64.1%, 72.4% and 63% inhibition activity against MCF-7 cells, respectively (**Fig. 3B** and **Suppl. Table 1**). MCF-7 is ER-dependent HER2-expressing [23, 24] and SkBR3 is ER-independent HER2 overexpressing cells [24, 25], while MDA-MB-231, and BT-549 are ER-negative HER2-negative cells ($HER2^-$) [26, 27]. Therefore, the results obtained indicated that compounds 12-14 are most likely selective against $HER2^+$ cell lines.

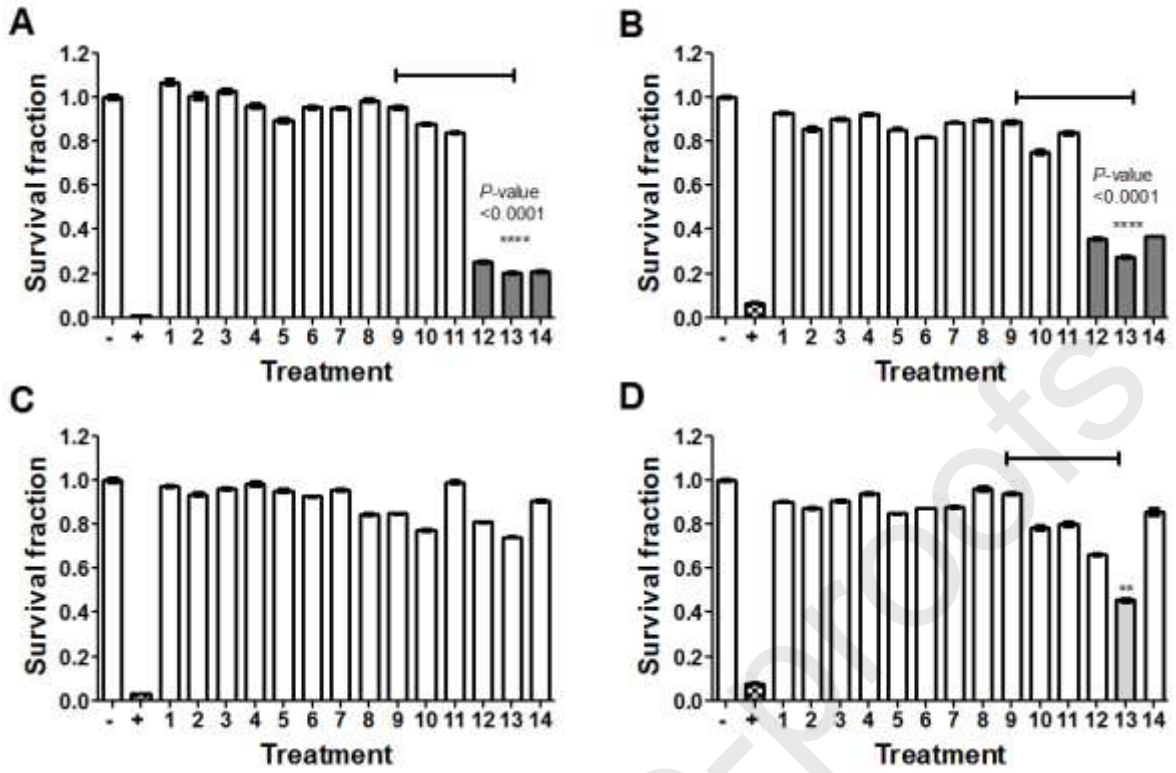

Fig 3. Cytotoxic effect of synthesized compounds on the survival of breast cancer cell lines including **A)** SKBr3, **B)** MCF-7, **C)** MDA-MB-231, and **D)** BT-549. The data was analyzed using one-way ANOVA and statistical significance was calculated using Dunnett's multiple comparisons test and the significance level indicated by asterisks (*****). The data display the mean ± SEM of 6 replicas.

The IC_{50} of compounds 12-14 against MCF-7 and SkBR3 was calculated (**Fig. 4, Table 1**). Compound 13 and 14 showed promising activity against SkBr3 at IC_{50} (0.73 ± 0.03µM) and (1.11 ± 0.3µM), respectively, while compound 13 and 12 showed promising activity against MCF-7 cell line at IC_{50} (1.3 ± 0.009µM) and (2.5 ± 0.19µM), respectively. To investigate the inhibitory activity of compounds 12-14 on the intracellular kinase domain of HER2, an ELISA assay was performed by measuring the ability of the compounds to inhibit the binding of epidermal growth factors to the kinase domain of HER2. HER2 detection antibody is known to specifically bind to the C-terminus kinase domain of HER2 [28]. The results obtained showed that compounds 12-14 at 10 µM caused >80% inhibition activity (**Table 2**).

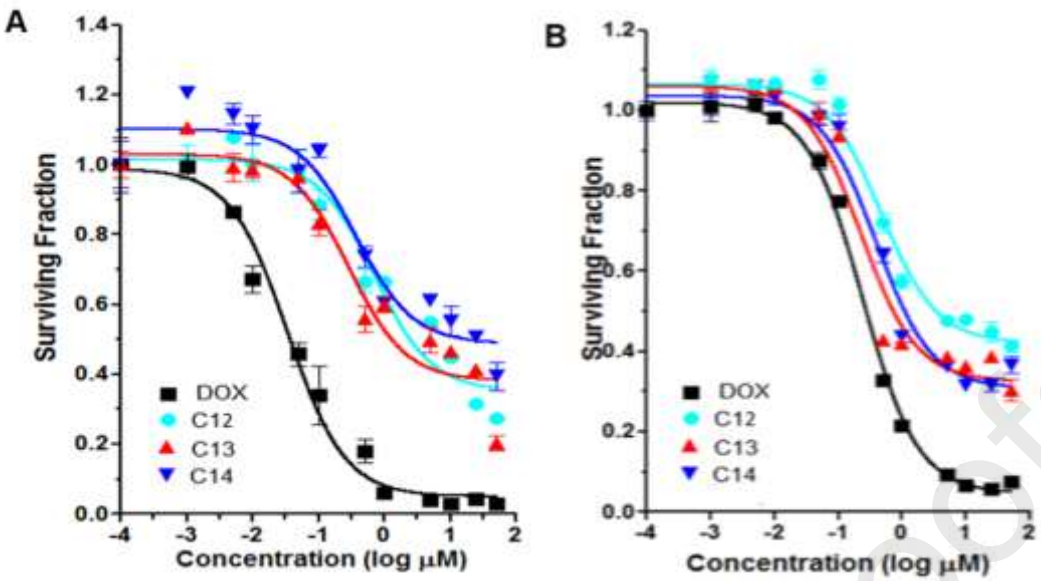

Fig.4. IC_{50} of compounds 12, 13 and 14 against A) MCF-7 and **B)** SkBr3.

Table 1. IC_{50} (μM) of compounds 12-14 against MCF-7 and SKBr3 cell lines.

Cp No.	MCF-7	SKBr3
Doxorubicin	0.035±0.002	0.28 ± 0.04
12	2.500±0.190	3.40 ± 0.40
13	1.300±0.010	0.73 ± 0.03
14	16.20±0.870	1.11 ± 0.30

The values represent the mean ± SEM of three independent experiments

Table 2. Percentage of HER2 inhibition by the newly-synthesized compounds at 10 μM.

Cp No	HER2
12	82.56±0.18
13	86.95±0.33
14	84.66±0.22

The values represent the mean ± SEM of three independent experiments

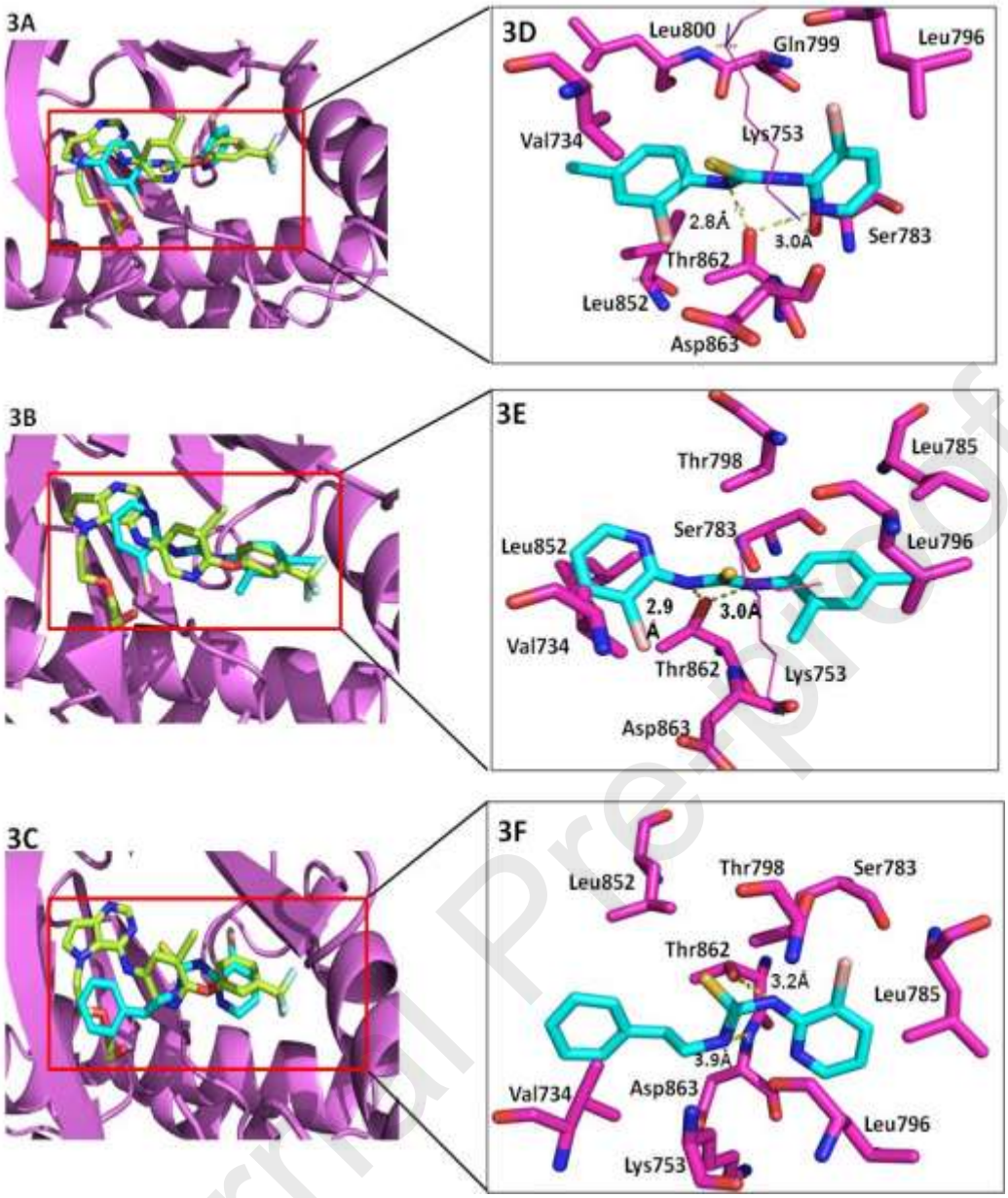

Fig. 5. Binding mode of compounds 12, 13, 14 (cyan), native ligand (green) (3A, 3B, 3C), respectively. Interaction of compounds 12, 13, 14 (cyan) with the key residue (magenta) (3D, 3E, 3F), respectively. HER2 represented as magenta cartoon.

Compared to the co-crystallized ligand (2-{2-[4-({5-chloro-6-[3-(trifluoromethyl) phenoxy] pyridin-3-yl}amino)-5H-pyrrolo[3,2-d]pyrimidin-5-yl]ethoxy}ethanol), compounds 12-14 were docked within the active site of HER2 protein (PDB: 3PP0) using AutoDock software. Re-docking the original ligand showed that it is co-crystallized with the HER2 protein at low RMSD value (<1Å) and formed three H-bonds with Met801, Thr862 and Asp863. Leu726, Lys753, Ala751, Ala771, Leu785, Leu796 and Leu852 contributed to the interaction by forming hydrophobic interactions, while Phe864 formed a π-π T-shaped

interaction (**Suppl. Table 2**). Similarly, compounds 12, 13 and 14 occupied the same position as the ligand within the active site of HER2 protein (**Fig. 5**). Compounds 12, 13 and 14 formed H-bonds with the key residue Thr862, while compound 14 formed an additional H-bond with Asp863. The three compounds showed π-π T-shaped interaction with Phe864 and hydrophobic interactions with the hydrophobic key residues Leu 726, Val734, Ala751, Lys753, Leu785, Leu796, Leu800 and Leu852 (**Fig. 5**).

Docking study of compounds 1-11 was carried out to investigate their interactions with the binding pocket and the main reason for their weak anticancer activity. Compound 1 with long chain linker, consisting of 7 atoms, showed H-bond between NH of urea moiety and the key residue Thr862. However, the extension of methoxy phenyl group out of the hydrophobic part of the binding pocket caused loss of the hydrophobic interactions with Leu726, Leu852 and Leu800 (**Supp. Fig. 1**). Urea derivatives in compounds 2 and 3 showed H-bond between NH of the urea moiety and Asp863 and Thr862, respectively. On the other hand, 3-flouro phenyl moiety of compound 2 and the 4-methoxy phenyl moiety of compound 3 were displaced away of the hydrophobic pocket. Replacement of urea moiety with thiourea in compounds 4-7 did not change the binding profile of the 4 compounds. Compounds 4, 5, and 7 showed H-bonds between NH of urea and Thr862, while caused poor fitting within the hydrophobic part of the pocket site, leading to reduced hydrophobic interactions. Compound 6 did not show neither H-bond nor hydrophobic interactions. Sulphonyl phenyl urea derivatives in compounds 8 and 9 showed H-bonds with Ser783 and Lys753, while showed poor binding in the hydrophobic pocket. Bromo-pyridine thiourea derivatives in compounds 10 and 11 showed H-bond with Thr862 and good binding within the pocket site. Collectively, it can be concluded that the good activity is related to the H-bonds formed with the key residues Thr862 and Asp863 and the hydrophobic interactions with the hydrophobic residues Leu852, Leu726 and Leu800, in addition to the π-π stacking with Phe864.

To evaluate the stability and flexibility of the docked complexes of compounds 12-14, molecular dynamics simulations were carried out for 50ns using GROMACS-5.2.1. Root mean square deviation (RMSD) values were plotted for APO protein, the native ligand and compounds 12-14 complexes within the active site of HER2 protein. The obtained RMSD graph showed that the three complexes formed with 12, 13 and 14 compounds reached equilibrium at 5ns with RMSD values 0.301, 0.262 and 0.263 nm, respectively (**Table 3**). All the three complexes were stable over the simulations run, while compound 14 underwent further conformational change lasted for additional few seconds prior to returning back to its

stable conformation. The native ligand complex also reached equilibrium at 5ns with RMSD value ~0.293 nm, while maintaining a sudden conformational change lasted for 10ns. On the other hand, APO protein showed two conformational statuses with RMSD value ~0.329 nm. All three 12, 13 and 14 complexes formed RMSD values lower than the APO protein alone, indicating that compounds 12, 13 and 14 formed stable interaction with the active site of the protein (**Fig. 6**). Compared to the native ligand RMSD value 0.08 nm, the mean RMSD values of the compounds 12, 13 and 14 were 0.087, 0.14 and 0.1 nm, respectively (**Table 3** and **Fig. 6**). The results obtained indicated that all three compounds formed stable complex within the active site of HER2 protein, while compound 12 was more similar to the native ligand.

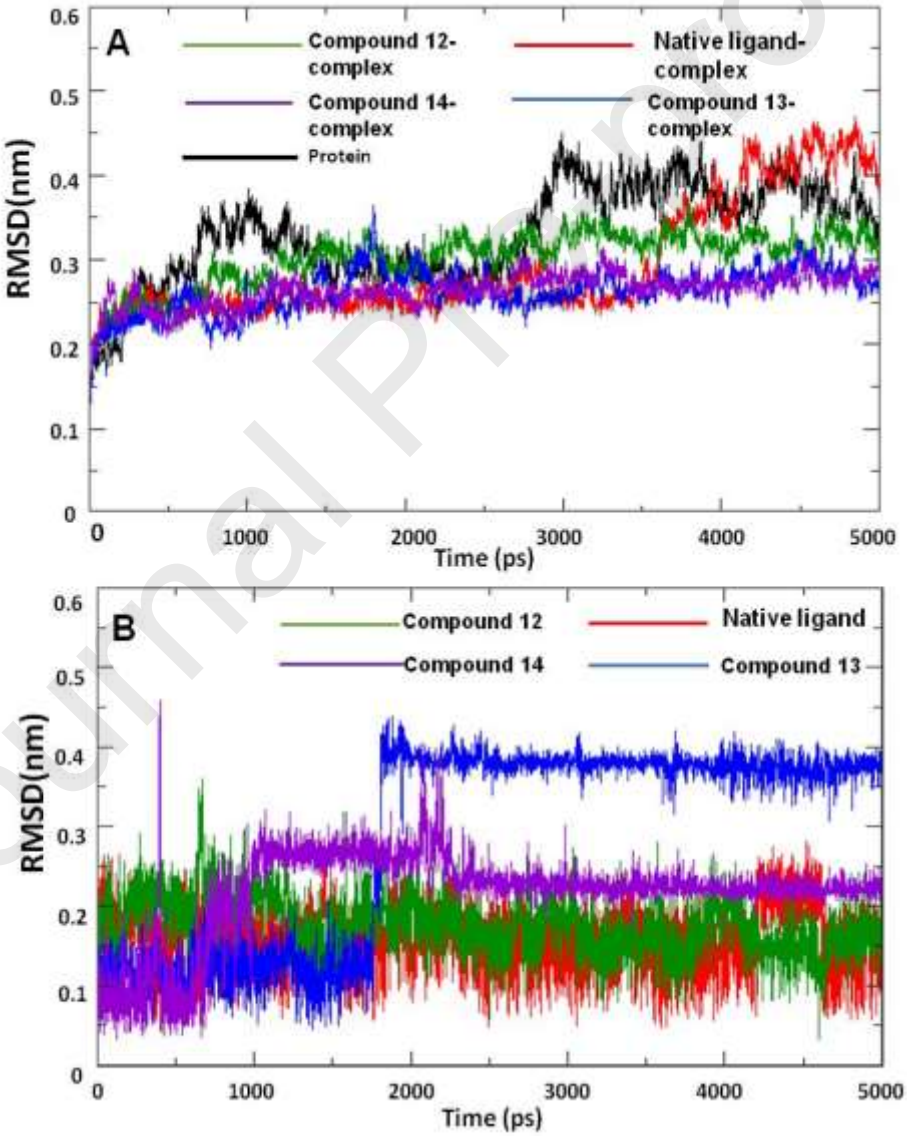

Fig. 6. (A) RMSD of compounds 12, 13, 14 and the native ligand when complexed with Cα of HER2 protein during a 50ns period. (B) RMSD of compounds 12, 13, 14 and native ligand during a 50ns period.

Table 3. Average values (nm) RMSD and RMSF for the native ligand and the compounds 12-14 complexes.

	protein	12	13	14	Native ligands
RMSD(complex)	0.329	0.301	0.262	0.263	0.293
RMSD (ligands)		0.087	0.14	0.1	0.080
RMSF	0.160	0.132	0.130	0.130	0.139
RMSF (pocket)	0.121	0.097	0.1047	0.102	0.1027

The root mean square fluctuation (RMSFs) of the residues of APO protein and the inhibitors-protein complexes were calculated over 50ns simulation period. The results showed an overlap of the plotted graphs of APO structure to HER2 protein and of the protein-ligands complexes. The average RMSF of the three complexes was lower than that of the Apo protein (0.13 nm versus 0.16nm) (**Table 3** and **Fig. 7A**). The stability of protein complexes was further evaluated by plotting the RMSF of the pocket residues (**Fig. 7B**). The highest amplitude of movement was occurred with the APO structure of HER2, which was attributed to the absence of ligand and hence retained a freedom in motion. On the other hand, the presence of inhibitors caused a decrease in the residue's amplitude of motion, within the range of 785-800, which was attributed to hydrophobic interactions of the inhibitors with the key residues Leu785, Leu796 and Leu800. Furthermore, the magnitude of movement of Leu852, Thr862 and Asp863 was decreased due to the hydrophobic interaction of leu852 with the ligands and the H-bond formed between Thr862 and Asp863 and the inhibitors. These results indicate that the inhibitors interactions with the residues of HER2 catalytic site influenced the protein dynamics and the inhibitory activity was related to the decrease in residues fluctuation within the pocket site.

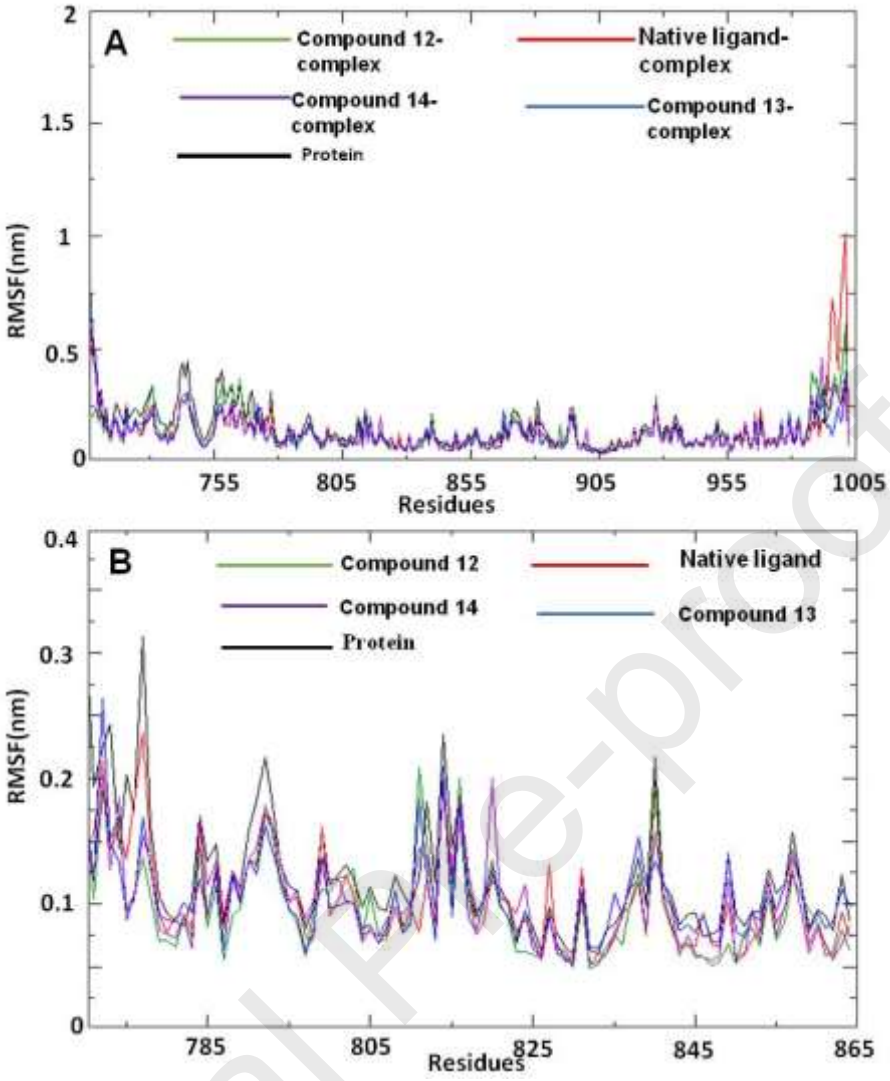

Fig. 7. (A) RMSF of compounds 12, 13, 14 and the native ligand when complexed with Cα HER2 during a 50ns period. (B) RMSF of compounds 12, 13, 14 and the native ligand in a complex with Cα of the pocket site residues of HER2.

To measure the compactness of protein, the radius of gyration (Rg) was calculated. The results obtained indicated that the three compounds showed static depiction with a constant Rg value at 1.97 nm throughout 50ns simulation period. On the other hand, the native ligand and APO protein depicts a variation at 3ns, followed by stability with Rg value 2.01 nm. These comparative results justified the better conformation of the three inhibitors-protein complexes when compared to the native ligand complex (**Suppl. Fig. 2**).

To confirm the stability of the compound-protein complex, the formation of H-bonds was analyzed over 50ns simulation period. The results showed that all the inhibitors-receptor

complexes formed at least one stable H-bond over the simulation period (**Suppl. Fig. 3**). Compound 12 formed two hydrogen bonds, which maintained most of the time. Compound 14 formed two H-bonds, while one of them was weak and formed only for 4ns. Compound 13 and the native ligand formed four bonds; three of them maintained most of the time. These results indicate that the H-bonds interactions between the inhibitor and HER2 played an important role in protein stabilization.

Hydrophobic interactions of the three inhibitors within the pocket site of HER2 receptor were visualized in MD trajectories using Pymol software. The results showed that residues Val734, Lys753, Leu785, Leu796, Leu800 and Leu852 were the common key hydrophobic contributors of the three inhibitors. **Suppl. Fig. 4** and **Suppl. Table 3** showed that the occupancy of the hydrophobic interactions of the key residues as a function of time was more than 90%. Based on the above results, hydrophobic residues near the binding pocket, including Val734, Lys753, Leu785, Leu796, Leu800 and Leu852 play an important role to the activity of the inhibitors.

To provide insight into the binding mechanisms between the inhibitors and HER2 receptor, the free binding energies were calculated by g_mmbsa method (**Suppl. Table 4**). The free binding energies of compounds 12, 13 and 14 were -107.43±0.64, -95.18±0.66, and -98.29±0.69 Kcal/mol, respectively. The contributions of van der Waals (ΔE_{vdw}), electrostatic (ΔEele), and non-polar solvation energies (ΔG_{nonpol}) were negative, while the contribution of polar free solvation energy (ΔG_{pol}) was positive, indicating that van der Waals, electrostatic and nonpolar interaction were favorable for the binding. Van der Waals (ΔE_{vdw}) was the greatest driving force that was contributed to the binding of inhibitor-protein active site.

To identify the residues important for the interactions, the free binding energy was decomposed into residues using MMPBSA.PY script (**Fig. 8**). The interaction profiles were quite similar with the three inhibitors 12, 13 and 14. Leu726, Val734, Lys753, Ala771, Leu785, Leu796, Leu852 and Phe864 residues contributed meaningfully with ~1.5 Kcal/mol energy. Leu796 (-6.2 Kcal/mol) contributed to the binding of compound 12, while Val734 (-6.0 Kcal/mol) contributed to the binding of compounds 13 and 14. Phe864 (-4.00, -5.00 and -2.7 Kcal/mol) contributed to the binding of compounds 12, 13 and 14, which can be attributed to the π-π interactions of Phe864 with the inhibitors. Leu785 and Leu852 contributed to the binding of the three compounds with an average binding energy -3.00 Kcal/mol. These three residues showed hydrophobic interactions with the inhibitors at high occupancy. In general, the results are in consistent with the hydrophobic interactions and the

calculated free binding energy. Most of the residues contributed in the binding energy were hydrophobic and utilized van der Walls interactions.

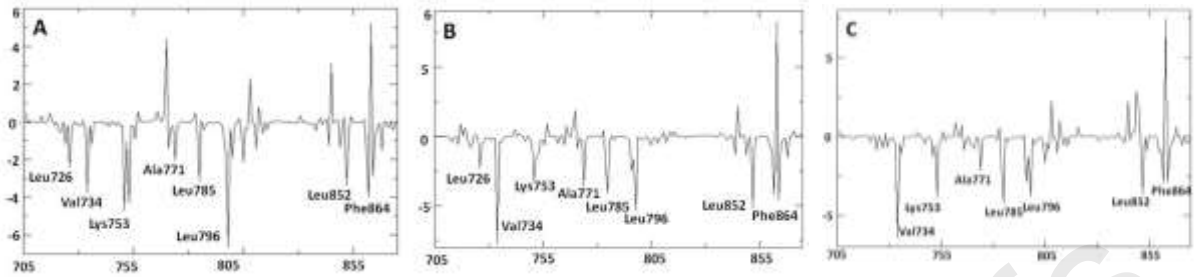

Fig. 8. Per-residue binding free energy decomposition of (A) Compound 12, **(B)** Compound 13, and **(C)** Compound 14.

To evaluate the drug-likeness and bioavailability of compounds 12, 13, and 14, ADME parameters of the compounds were calculated using SwissADME web tool (**Table 4**). The results showed that the three compounds formed H-bond donors ≤ 5 and acceptors ≤ 10 as stated with Lipinski rule, indicating that the compounds are ionizable and subsequently their solubility and absorption are adequate. The log *P*-values of the compounds were in the range of 3.33- 4.16, and the log *S*-values were ≤ 6, indicating that they have reasonable solubility and good absorbance, which is confirmed with the good calculated intestinal absorbance (**Table 4**). Lower TPSA values of the compounds (69.04 A^2) suggested that they have better cellular internalization properties. Moreover, compounds 12-14 showed an inhibitory effect on cytochrome CYP1A2, indicating that they have a prolonged action and good therapeutic effect. In conclusion the three compounds comply with Lipinski rules and drug-likeness parameters.

Table 4. ADME prediction of compounds 12, 13 and 14.

No	Log P	TPSA A^2	Log S	Rotatable bonds	HBD	HBA	CYP1A2 inhibition	GI A	Lipinski filter
12	4.16	69.04	-5.40	4	2	1	Yes	Yes	Yes (0 violation)
13	4.07	69.04	-5.09	4	2	1	Yes	Yes	Yes (0 violation)
14	3.33	69.04	-4.16	6	2	1	Yes	Yes	Yes (0 violation)

*TPSA: total polar surface area, GI A: Gastrointestinal absorbance, HBD: Hydrogen bond donor, HBA: Hydrogen bond acceptor.

The bioavailability radars of the three inhibitors were represented in **Fig. 9**. The pink areas identify the optimum range of six properties, namely flexibility, lipophilicity, size, polarity, insolubility, and instauration. The three compounds were almost within the range of conformity, while in the instauration property, the fraction of carbons in the sp3 hybridization is increased from 0.25 to a higher value. In general, the pharmacokinetic properties of the three designed compounds are acceptable.

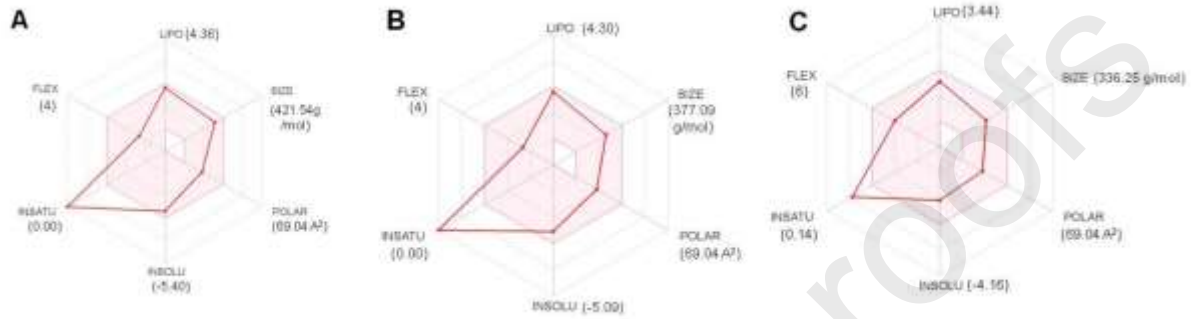

Fig. 9. The bioavailability radars of compounds (A) 12, (B) 13, and (C) 14. The pink areas identified the optimum properties range. The three compounds were within the range of conformity, and with accepted pharmacokinetics.

3D QSAR models were carried out using open3dqsar software using a training set of 11 molecules, and a test set of 3 molecules against MCF-7. The result was represented graphically by scattering plots of the experimental activity against predicted activity (**Table 5, 6** and **Suppl. Fig. 5**). The results from the PLS analysis showed a squared correlation coefficient r^2 =0.9966, cross validation q^2 = 0.4010 for five components, r^2 predicted = 0.40 and SDEC = 0.0307. PLS statistics of the predicted and expected activity (**Table 5**) indicated the reliability and productivity of the CoMFA model.

Table 5. Observed and predicted activities of the training set against MCF-7 cell line by 3D QSAR.

Cp NO	Observed activity (*p*)	Log *p*/(100-*p*)	Predicted activity 3D QSAR model
1	7.235	-1.107	*
2	14.45	-0.7723	-0.76
3	9.910	-0.9586	-0.94

4	7.870	-1.0684	-1.05
5	14.61	-0.7667	*
6	18.00	-0.658	-0.65
7	11.32	-0.8939	*
8	10.30	-0.9399	-0.94
9	11.17	-0.9005	-0.91
10	24.85	-0.4806	-0.48
11	16.19	-0.7100	-0.71
12	64.08	0.2513	0.32
13	72.39	0.4084	0.33
14	63.00	0.231	0.26

To validate the constructed 3D QSAR models, 3 compounds (1, 5 and 7) were used as a test set, and their biological values were predicted from PLS equation derived from CoMFA model. The obtained average deviation between experimental and predicted values was small, suggesting that 3DQSAR model give a good prediction regarding the estimation of the activity of the novel compounds (**Table 6**).

Table 6. Observed and predicted activities of the test set against MCF-7 cell line by 3D QSAR.

Cp No	Observed activity	Predicted activity
1	-1.10	-0.62
5	-0.76	-0.86
7	-0.89	-1.08

CoMFA steric map of compounds 12, 13 and 14 was illustrated in **Fig. 10A-C**. The steric interactions were represented by green for the favored steric substituent, and yellow for the unfavored steric substituent. Compounds 12, 13 and 14 showed the same steric contour maps. A large green contour surrounded by bromide atom in 3-bromo-pyridine and extended to positions 4 and 5 of the pyridine ring was observed, which indicated that bulky group was preferred in position 3 of the pyridine ring. Addition of substituent at position 4 and 5 improved the inhibitory activity of the compounds. Another green contour map found near 4-Cl atom of 4-chloro phenyl ring of the compounds 12, and 13, suggesting that the presence of bulky groups in this position may be a factor to enhance the activity of both compounds.

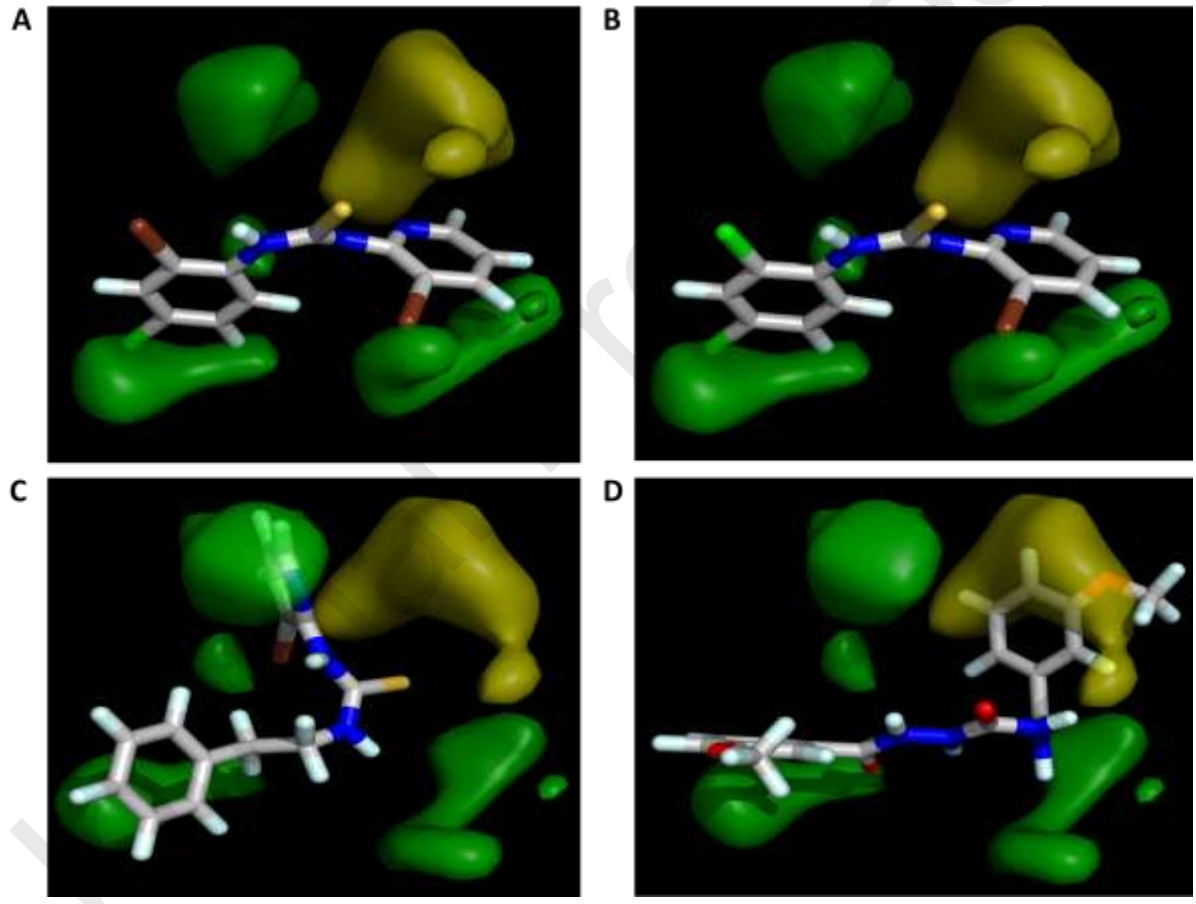

Fig. 10. CoMFA steric contours map of the active compounds (A) Compound 12, **(B)** Compound 13, and **(C)** Compound 14 versus less active compound **(D)** Compound 1. Sterically favored areas are shown in green colors, while sterically unfavored areas are shown in yellow**.**

To validate the data, a less active compound (compound 1) was employed as control. A large yellow contour map was located around 3-methoxy group of the phenyl ring of the

compound, suggesting that groups with low steric factor are required for the activity (**Fig. 10D**). This may explain the reason why compound 1 is less potent against MCF-7 cell line.

The CoMFA electrostatic contour plots of the most active compounds (12-14) were displayed in **Fig. 11A-C**. A blue contour indicated that the electropositive substituent was favored, while the red colour indicated that the electron-rich substituent was preferred. Since the blue contour was overlapping the NH between the pyridine and C=S in the three active compounds, the presence of nitrogen is essential for the activity. There were another two blue contours near the un-substituted 3 and 5 position of the phenyl ring of compounds 12 and 13 indicating that the addition of electron deficient groups in these positions can increase the binding affinity and hence the inhibitory activity (**Fig. 11**). Compound 14 showed two blue contours, one around the un-substituted position of phenyl ring and CH_2CH_2 groups, which indicated that the addition of electropositive groups at these positions will increase the activity. The red contour maps in compounds 12 and 13 surrounding the 3-bromo pyridine ring explained that the presence of electronegative group such as Br is important for the activity, while the red contour in compound 14 overlapping the C=S group indicated that the electronegative group is preferred.

CoMFA electrostatic map of the less potent compound 1 (**Fig. 11D**) showed two large blue contours around the two C=O groups in compound 1, which indicated that the electronegative groups were unfavorable in this position. This may explain why compound 1 is less active. The two blue contours around NH and CH_2 indicated that the NH is important for the activity. The results are in alignment with CoMFA results of compounds 12-14. However, it is better for the activity to add electropositive group to the CH_2 group. The red contour overlapping C=O group, which connected to the phenyl group, indicated that the electronegative group is favorable.

Based on the results obtained from the 3D QSAR, the presence of bulky electronegative group in position 3 of pyridine ring and position 4 of phenyl ring is important for the activity. Furthermore, the presence of electropositive group such as nitrogen atom in the linker between the two aromatic rings is important for the activity. The addition of electropositive groups in position 3 and 5 of phenyl ring is important for the activity.

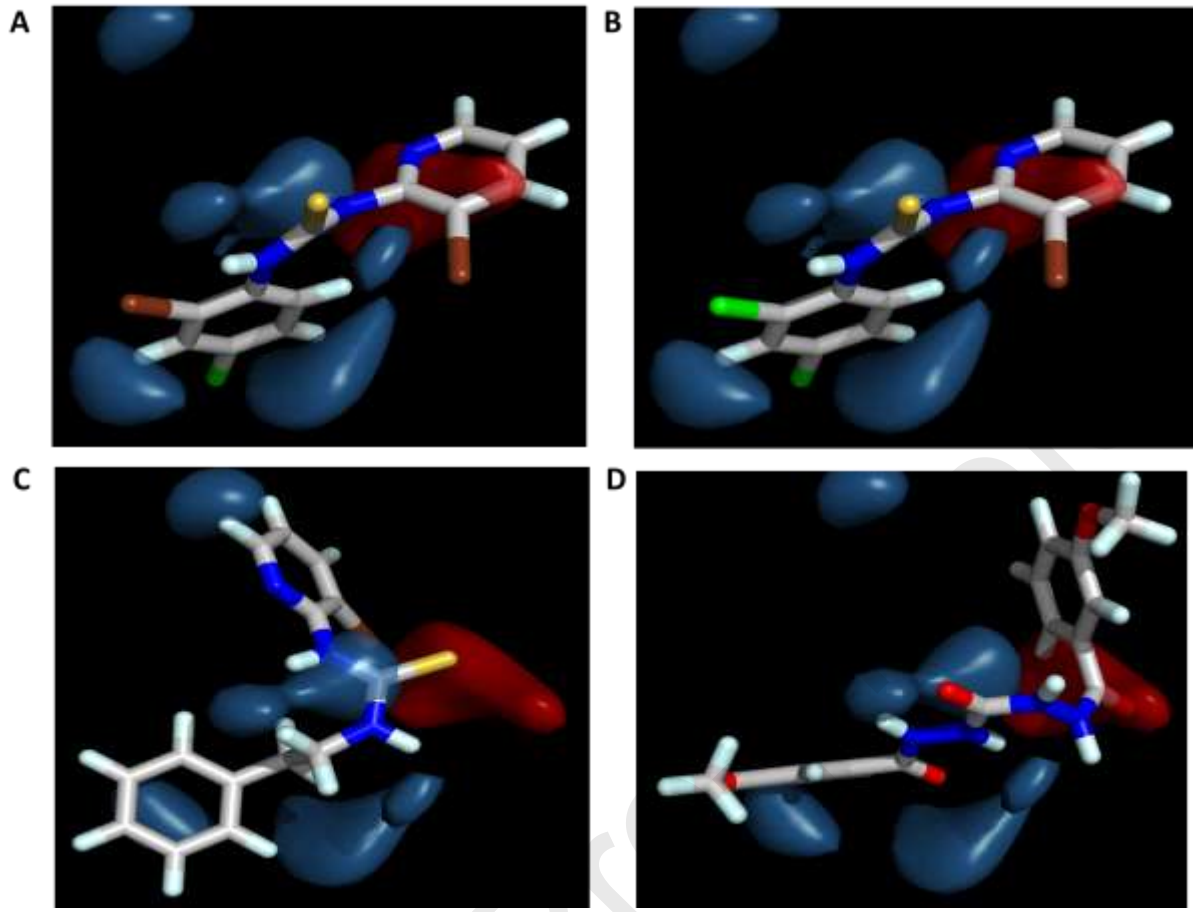

Fig. 11. CoMFA electrostatic contours map of active compounds (A) Compound 12, **(B)** Compound 13, and **(C)** Compound 14 versus less active compound **(D)** Compound 1. Electron-deficient favored areas are shown in blue colors, while electron-rich favored areas are shown in red.

Human epidermal growth factor receptor 2 (HER2) is overexpressed in ~ 15%- 30% of breast cancers and is generally associated with low patient survival [1-3]. Although the normal expression of HER2 is important for the regulation of cell growth and cell proliferation, its overexpression is indicative of aggressive metastatic breast cancer [4]. Until now, there is no natural ligand identified for HER2. HER2 dimerizes with another member of epidermal growth factor receptor family to form a potent heterodimer, despite its inability to directly bind with a specific ligand [5]. Two clinical approaches were adopted for the inhibition of HER2-positive breast cancers, the use of monoclonal antibodies or tyrosine kinase inhibitors [6]. The development of resistance to the FDA-approved monoclonal antibody, trastuzumab (Herceptin®) [7], initiated the research focus in the development of inhibitors to

$HER2^+$ breast cancer including in particular by selective targeting of the tyrosine kinase domain of HER2.

Different scaffolds have been developed as HER2 inhibitors including anilinoquinazolines [8], pyrrolotriazinamines [9], pyrrolopyrimidines [9] and pyrimidoazepines [10]. Although they target HER2, their main drawback is associated with their non-selective targeting of the tyrosine kinase. Lapatinib (Tykerb/Tyverb®) is an anilinoquinazolines FDA-approved reversible dual EGFR/HER2 inhibitor. Although the drug showed promising results in phase I& II clinical trials, soon it developed resistance [11]. Further, afatinib (Gilotrif/Giotrif®), an approved drug used in the treatment of metastatic non-small cell lung carcinoma (NSCLC) and its activity against metastatic breast cancer is still under investigation, shows high toxicity profile [12]. Furthermore, other developed kinase inhibitors are either show high toxicity profiles or their therapeutic potential is still unconfirmed [13]. Therefore, there is a need to develop new structural scaffold inhibitor, targeting HER2 kinase.

Here, we aim to design and synthesize small molecules that selectively bind and inhibit HER2. Based on the availability of HER2 crystal structure and the annotation of the key residues, a series of diaryl urea/ thiourea scaffolds were developed as isostere of known HER2 inhibitors including Linifanib and Sorafenib. The new compounds, arylthiosemicarbazide scaffold, exhibited potent HER2 inhibition activity with promising IC_{50}. Compounds 1-14 were screened against breast cancer cell lines. Only compounds 12-14 showed promising activity against SKbr3 and MCF7, $HER2^+$ cancer cells, but not MDA-MB-231, and BT-549, $HER2^-$ cancer cells, indicative of selective inhibition activity. Although compounds 3-8 and 14 were previously reported [29], their anti-breast cancer activity was never investigated. This is considered as the first report for the activity of arylthiosemicarbazide scaffold against breast cancer cells by selectively targeting HER2. Further, to confirm the selectivity of compounds 12-14 against HER2- kinases, compounds 12-14 were docked against different kinases. As shown in **Table 7**, the lowest binding score was identified against HER2 kinase, indicative of kinase selectivity. A future study to investigate the kinases selectivity of more derivatives of compounds 12-14 will be conducted.

Table 7. Binding score of compounds 12-14 against several kinases in Kcal/mol

Kinases	Compound 12	Compound 13	Compound 14
HER2 (PDB:3PP0)	-5.7	-5.1	-5.6
p38 MAPK kinase (PDB: 3FMK)	-4.8	-4.2	-4.4

C Src (PDB:4U5J)	-2.9	-3.4	-2.3
B-Raf (PDB:3C4C)	-4.5	-4.2	-4.1

Aligning the catalytic domains of 65 protein kinases revealed the identification of 11 subdomains with a conserved signature motif DFG(Asp-Phe-Gly) [30]. The configuration of DFG motif controls the substrate binding and catalysis [31]. It has been shown that kinase enzymes have two conformations, inactive and active forms. The inactive form "DFG out" where the Aspartate is directed out from the active site, while the active form "DFG-D in" configuration where the Aspartate is directed into the active site [32]. Protein kinase inhibitors are three classes, type I inhibitors are those bind to the active conformation (DFG- in) of ATP pocket, type II inhibitors bind to the inactive form (DFG-out) of ATP pocket, while type III inhibitors are known as non-ATP competitive inhibitors as the compounds bind to allosteric site [33]. According to our docking and molecular dynamics studies, compounds 12-14 bind to DFG in the HER2 ATP conformation binding site. Further, the Aspartate residue of DFG in the three molecules is directed towards the binding pocket and DFG-in motif is in its active form, indicating that the three molecules are mostly type I kinase inhibitor. A future experiment will be conduct to confirm the aforementioned data using several derivatives of compounds 12-14.

The conserved occurrence of kinase domains challenges the development of selective inhibitor to HER2 kinase. Availability of enzyme crystal structures and computational studies including molecular modelling, docking and simulations helped to identify the key residues in the active site of the target protein required in the binding interaction, and hence validate the efficient and selective inhibition activity of the newly-designed compounds [34]. Extensive computational studies were carried out for the potential anti-breast cancer compounds 12-14 against HER2 protein compared to those showed no activity. Molecular docking indicated that compounds 12-14 formed H-bond with the key residues Thr862, pi-pi stacking with Phe864 and hydrophobic interactions with the key hydrophobic residues, which can explain their high binding affinity to HER2. Molecular dynamics simulation confirmed the stability of HER2 protein-compounds complexes during 50 ns, indicating the fitting of compounds 12-14 within the binding pocket of HER2. Calculation of the binding energy was carried out and it showed that Van-der Waals interaction is the major force responsible for the binding of the compounds within the receptor.

Compounds 1-11 showed weak to moderate inhibitory activity against the tested cancer cell lines. The methoxy phenyl carbohydrazide derivative in compound **1,** which contained a long hydrophilic chain of 7 atoms as linker showed low anticancer activity against the four cancer cell lines. When the length of the linker was shortened to 5 atoms in compounds 2 and 3, the inhibitory activity against MCF-7 cancer cell line was slightly improved to 14.5±0.025 and 10.0±0.009 %, respectively. Generally, the replacement of urea moiety with thiourea in compounds 5-7 improved the inhibitory activity against cancer cells when compared to the urea derivatives in compounds 1-3. However, the replacement of 3-methoxy-4-hydroxy phenyl substituent of compound 4 with 2-methoxy substituent improved the inhibitory activity to 11% as in compound 5. Addition of ethyl substituent to the N-atom in the thiourea moiety and the replacement of methoxy substituent with H-atom increased the inhibitory activity of compound 6 against MCF-7 (18.00±0.010%) and BT549 (12.60±0.004%), while decreased the inhibitory activity against SKBr3 to 4.9%. Replacement of phenyl group of compounds 5 and 6 with pyridine group and addition of chlorine substituent in the *p*-position of phenyl group reduced the inhibitory activity of compound 7 against the cancer cell lines. The addition of sulphonyl urea moiety as linker between the two aromatic groups improved the inhibitory activity of compound 8 against MDA-MB-231 to ~ 15%. Merging 3-bromopyridine with thiourea linker and reducing the number of connector atoms improved the inhibitory activity of compounds 10 and 11 against MCF-7 and BT547 to ~ 20% and against SKBr3 to ~14%.

Compounds 12-14 with thiourea connector and bromopyridine heterocycle showed up to 70% inhibitory activity against MCF-7 and SKBr3 with promising IC_{50}. These results indicated that the short linker, and the presence of bromopyridine moiety and 2, 4 substituted phenyl groups are important for the anticancer activity. Therefore, we can conclude that compounds 12-14 are efficient and selective binding inhibitors to HER2 kinase protein.

In conclusion, following a process of discovery for selective anticancer drugs against breast cancers, we have designed and synthesized 14 compounds. Out of the 14 compounds, compounds 12-14 showed selective anticancer activities against HER^+ cells including in particular SkBr33 and MCF-7 cancer cell lines. Compounds 12-14 showed IC_{50} (3.40 ± 0.40, 0.73±0.03, 1.11 ± 0.30) µM, respectively against SKBr3 and (2.500±0.190, 1.300 ±0.03, 16.20±0.870) µM, respectively against MCF-7. Compounds 12-14 at 10 µM showed ≥ 80%

inhibition activity to HER2 kinase. Computational analyses using molecular docking, molecular dynamics, binding energy calculations and 3DQSAR models were employed to validate the selectivity of the compounds. Molecular docking and MD simulations showed the formation of strong hydrogen bond with the key residue (Thr862), pi–pi stacking interactions with the key residue (Phen864) and hydrophobic interactions with Val734, Leu785, Leu800 and Leu852, indicative of their critical roles in the binding of the compounds with the receptor. Calculation of the binding energy revealed that Van-der Waals interaction is the major force responsible for the binding of the compounds with the receptor. The residue decomposition results confirmed the importance of Val 734, Leu796 and Phe864 in the binding of compounds 12-14. The results from the molecular docking and MD simulations, and calculation of the binding energy were consistent. 3DQSAR was developed to discover the key structural factors that influence the anticancer activities. The results from 3DQSAR showed that 3-Br substituted pyridine ring and 3-Cl substituted phenyl ring are important for the activity. The NH group in the linker, connecting the two-aryl groups, showed essential role for the activity and selectivity. Furthermore, ADMET results confirmed that the three compounds comply with Lipinski rules and drug-likeness. Our results indicated that we have developed novel selective, effective and safe novel anti-breast cancer agents, which deserve further pre-clinical development.

Declaration of Competing Interest

The authors declare no conflicts of interest.

Appendix A. Supplementary data

Supplementary data to this article can be found online.

References

1. Das D, Xie L, Wang J, et al. Discovery of new quinazoline derivatives as irreversible dual EGFR/HER2 inhibitors and their anticancer activities – Part 1. *Bioorganic & Medicinal Chemistry Letters.* 2019;29(4): 591-596.
2. Milik S, Abdel-Aziz A, Lasheen D, Serya R, Minucci S, Abouzid K. Surmounting the resistance against EGFR inhibitors through the development of thieno[2,3-d]pyrimidine-

based dual EGFR/HER2 inhibitors. *European Journal of Medicinal Chemistry.* 2018;155: 316–336.

3. Ignatiadis M, Desmedt C, Sotiriou C, de Azambuja E, Piccart M. HER-2 as a Target for Breast Cancer Therapy. *Clinical Cancer Research.* 2009;15(6): 1848-1852.
4. Whenham N, D'Hondt V, Piccart MJ. HER2-Positive Breast Cancer: From Trastuzumab to Innovatory Anti-HER2 Strategies. *Clinical Breast Cancer.* 2008;8(1): 38-49.
5. Li E, Hristova K. Role of Receptor Tyrosine Kinase Transmembrane Domains in Cell Signaling and Human Pathologies. *Biochemistry.* 2006;45(20): 6241-6251.
6. Gutierrez C, Schiff R. HER2: biology, detection, and clinical implications. *Arch Pathol Lab Med.* 2011;135(1): 55-62.
7. Engel RH, Kaklamani VG. HER2-positive breast cancer: current and future treatment strategies. *Drugs.* 2007;67(9): 1329-1341.
8. Steffensen KD, WaldstrØm M, Jeppesen U, Jakobsen E, Brandslund I, Jakobsen A. The prognostic importance of cyclooxygenase 2 and HER2 expression in epithelial ovarian cancer. *International Journal of Gynecological Cancer.* 2007;17(4): 798-807.
9. Eskens FALM, Mom CH, Planting AST, et al. A phase I dose escalation study of BIBW 2992, an irreversible dual inhibitor of epidermal growth factor receptor 1 (EGFR) and 2 (HER2) tyrosine kinase in a 2-week on, 2-week off schedule in patients with advanced solid tumours. *Br J Cancer.* 2008;98(1): 80-85.
10. Okarvi SM, AlJammaz I. Development of the Tumor-Specific Antigen-Derived Synthetic Peptides as Potential Candidates for Targeting Breast and Other Possible Human Carcinomas. *Molecules.* 2019;24(17): 3142.
11. Capala J, Bouchelouche K. Molecular imaging of HER2-positive breast cancer: a step toward an individualized 'image and treat' strategy. *Curr Opin Oncol.* 2010;22(6): 559-566.
12. Li H-Q, Lv P-C, Yan T, Zhu H-L. Urea Derivatives as Anticancer Agents. *Anti-cancer agents in medicinal chemistry.* 2009;9: 471-480.
13. Procopio G, Verzoni E, Testa I, Nicolai N, Salvioni R, Debraud F. Experience with sorafenib in the treatment of advanced renal cell carcinoma. *Ther Adv Urol.* 2012;4(6): 303-313.
14. Aversa C, Leone F, Zucchini G, et al. Linifanib: current status and future potential in cancer therapy. *Expert Review of Anticancer Therapy.* 2015;15(6): 677-687.

15. Li H-Q, Yan T, Yang Y, Shi L, Zhou C-F, Zhu H-L. Synthesis and structure–activity relationships of N-benzyl-N-(X-2-hydroxybenzyl)-N′-phenylureas and thioureas as antitumor agents. *Bioorganic & Medicinal Chemistry.* 2010;18(1): 305-313.
16. Widiandani T, Meiyanto E. Docking and Antiproliferative Effect of 4-T-Butylbenzoyl-3-Allylthiourea on MCF-7 Breast Cancer Cells With/Without Her-2 Overexpression. *SSRN Electronic Journal.* 2019.
17. Gogoi D, Baruah VJ, Chaliha AK, Kakoti BB, Sarma D, Buragohain AK. 3D pharmacophore-based virtual screening, docking and density functional theory approach towards the discovery of novel human epidermal growth factor receptor-2 (HER2) inhibitors. *Journal of Theoretical Biology.* 2016;411: 68-80.
18. Elseginy SA, Lazaro G, Nawwar GAM, Amin KM, Hiscox S, Brancale A. Computer-aided identification of novel anticancer compounds with a possible dual HER1/HER2 inhibition mechanism. *Bioorganic & Medicinal Chemistry Letters.* 2015;25(4): 758-762.
19. Bronte G, Andreis D, Bravaccini S, et al. Sorafenib for the treatment of breast cancer. *Expert Opinion on Pharmacotherapy.* 2017;18(6): 621-630.
20. Moreno-Aspitia A. Clinical overview of sorafenib in breast cancer. *Future Oncology.* 2010;6(5): 655-663.
21. Widiandani T, Meiyanto E. Docking and Antiproliferative Effect of 4-T-Butylbenzoyl-3-Allylthiourea on MCF-7 Breast Cancer Cells With/Without Her-2 Overexpression. *E, Docking and Antiproliferative Effect of.* 2019.
22. El-Awady RA, Semreen MH, Saber-Ayad MM, Cyprian F, Menon V, Al-Tel TH. Modulation of DNA damage response and induction of apoptosis mediates synergism between doxorubicin and a new imidazopyridine derivative in breast and lung cancer cells. *DNA Repair.* 2016;37: 1-11.
23. Kumar R, Mandal M, Lipton A, Harvey H, Thompson CB. Overexpression of HER2 modulates bcl-2, bcl-XL, and tamoxifen-induced apoptosis in human MCF-7 breast cancer cells. *Clinical Cancer Research.* 1996;2(7): 1215-1219.
24. Lattrich C, Juhasz-Böss I, Ortmann O, Treeck O. Detection of an elevated HER2 expression in MCF-7 breast cancer cells overexpressing estrogen receptor β1. *Oncology reports.* 2008;19: 811-817.
25. Seo HS, Ku JM, Choi HS, et al. Apigenin induces caspase-dependent apoptosis by inhibiting signal transducer and activator of transcription 3 signaling in HER2-overexpressing SKBR3 breast cancer cells. *Molecular medicine reports.* 2015;12(2): 2977-2984.

26. Watanabe S, Yonesaka K, Tanizaki J, et al. Targeting of the HER2/HER3 signaling axis overcomes ligand-mediated resistance to trastuzumab in HER2-positive breast cancer. *Cancer Med.* 2019;8(3): 1258-1268.
27. Dai X, Cheng H, Bai Z, Li J. Breast Cancer Cell Line Classification and Its Relevance with Breast Tumor Subtyping. *J Cancer.* 2017;8(16): 3131-3141.
28. Fu W, Wang Y, Zhang Y, et al. Insights into HER2 signaling from step-by-step optimization of anti-HER2 antibodies. *MAbs.* 2014;6(4): 978-990.
29. Lind PT, Morin Jr J, Noreen R, Ternansky R. Thiourea derivatives and methods for inhibition of HIV and related viruses. *Chemical Abstract.* 1993:160110.
30. Hanks SK, Quinn AM, Hunter T. The protein kinase family: conserved features and deduced phylogeny of the catalytic domains. *Science.* 1988;241(4861): 42-52.
31. Meharena HS, Chang P, Keshwani MM, et al. Deciphering the structural basis of eukaryotic protein kinase regulation. *PLoS Biol.* 2013;11(10): e1001680.
32. Huse M, Kuriyan J. The conformational plasticity of protein kinases. *Cell.* 2002;109(3): 275-282.
33. Monod J, Changeux J-P, Jacob F. Allosteric proteins and cellular control systems. *Journal of molecular biology.* 1963;6(4): 306-329.
34. Schroeder RL, Stevens CL, Sridhar J. Small molecule tyrosine kinase inhibitors of ErbB2/HER2/Neu in the treatment of aggressive breast cancer. *Molecules.* 2014;19(9): 15196-15212.

Highlights

- New compounds with specific targeting to HER2 receptor are designed.
- The compounds target only the $HER2^{+}$ cells.
- Computational modeling proved the specificity of the developed structures**.**